Parametric analysis on the performance of a revolutionary rotary Ericsson heat pump/engine

Wenbin Zhang[1,3*], Chris Benson[1], Andrew Cunningham[2] and Saffa Riffat[1]

[1]Department of Architecture and Built Environment, The University of Nottingham, University Park, Nottingham, UK, NG7 2RD; [2]Geo Green Power Ltd, Green Barn, Costock Road, Wysall, Nottinghamshire, UK, NG12 5QT; [3]School of Engineering and Technology, University of Hertfordshire, Hatfield, Hertfordshire, UK, AL10 9AB

Abstract

A revolutionary mechanical heat pump/engine system utilizing the Ericsson thermodynamic cycle has been proposed to provide efficient and environmentally friendly cooling. Computer simulation models have been developed to simulate the rotor positions. Further modeling has been conducted to predict the torque and power of the rotary Ericsson heat pump (REHP). Parametric and optimization study has been conducted to evaluate the factors affecting the mechanical and thermal performance of the conceptually designed REHP. It has been found that the rotor size, compression ratio and base pressure are the factors determining the maximum torque and power of the Motor-Generator (MG).

Keywords: heat pump/engine; Ericsson; computer simulation; parametric analysis

*Corresponding author:
w.zhang22@herts.ac.uk

Received 25 April 2018; revised 17 November 2018; editorial decision 24 November 2018; accepted 27 November 2018

1 INTRODUCTION

The 2008 Climate Change Act established the world's first legally binding climate change target. The UK government aims to reduce the UK's greenhouse gas emissions by at least 80% (from the 1990s baseline) by 2050 [1]. Moving to a more energy efficient, low-carbon economy will help to meet this target. It will also help the UK become less reliant on imported fossil fuels and less exposed to higher energy prices in the future.

The majority of coolers, refrigerators and air conditioners today are based on the vapor compression cycle using HFC's (Freon). Although efficient, the use of HFC's has significant detrimental environmental issues and its discontinued use is mandated [2]. Industry has yet to find a satisfactory replacement for such systems. Stirling coolers with just slightly more efficiency than today's would immediately fill this extremely large market. The need for improved energy performance and replacing refrigerants, together with tackling issues such as noise and recyclability will see the UK refrigeration market total 1.1bn UK Pounds in 2016 [3]. In thermodynamics, a heat engine is a reversible system of heat pump that performs the conversion of heat or thermal energy to mechanical work [4]. The world's need for an extremely low maintenance, highly efficient engine able to draw energy from solar, geothermal, waste heat and most any fuel is manifest. Extremely large markets would be open as soon as research and development allows.

A thermodynamic cycle represents an idealized mechanical engine. The Carnot cycle, the most efficient cycle that could be executed between a constant temperature heat source and constant temperature heat sink, is the ideal cycle for a heat pump. Whilst only being theoretical, it is used as a benchmark against which other heat pumps are compared. Two cycles, that in their ideal forms can achieve Carnot efficiency, are the Stirling and Ericsson cycles, which may be operated as heat engines, or, in reverse, as heat pumps. Both are very similar in having isothermal compression and expansion sections, yet differ in regeneration of heat in the Stirling's isochoric sections and the Ericsson's isobaric sections. In real mechanical systems, isothermal

doi:10.1093/ijlct/cty055 Advance Access Publication 21 December 2018

compression and expansion plus complete regeneration is very difficult to achieve [5]. Further heat exchangers are required to add and remove heat, making the cycle efficiencies comparable to other cycles (e.g. Rankine) and certainly not approaching Carnot efficiency. The Stirling cycle potential is reduced because of the clearance spaces, especially around the regenerator, which must have significant volume to maximize the heat exchange area, yet is un-swept by the piston, greatly reducing efficiency and power [6]. The Ericsson cycle has significant advantages over the Stirling cycle. In particular, it avoids the 'dead' volume of the Stirling system by using a double-acting mechanical configuration and replaces the Stirling 'regenerator' by a simple counter flow heat exchanger, the 'recuperator' for internal heat recovery, providing a simpler design. A most important advantage of the Ericsson engine is its modularity with sections of the cycle separated by valves, which means that each part of the engine can be studied and optimized separately, before being inserted in the whole engine. Kaushik [5, 7] obtained Ericsson engine performances comparable to the Stirling engine, while Wojewoda [8] showed that Ericsson cycle performance can be better than the Stirling cycle, at least in some cases [9]. In both machines, isothermal compression or expansions were not achievable due to the insufficient heat transfer area during the compression and expansion sections. Nevertheless, a properly designed Ericsson cycle heat pump has the potential to achieve near-isothermal operation, a contention supported by the work of Caelsen [10] on Stirling machines.

Despite its advantages over the Stirling cycle, few papers address Ericsson machines, including for combined heat and power (CHP) energy where it might be especially advantageous. The literature includes an Engineering Equation Solver (EES) modeling of compressor and expander liquid flooding to approach isothermal compression and expansion in a cooler [11, 12]. The authors concluded that in the ideal case, the COP approaches Carnot as the liquid flooding is increased, but in the non-ideal case the rotating machinery introduced significant irreversibility. A further useful study of the Ericsson cycle [6] has established relationships between the geometrical characteristics of an Ericsson engine, its operating parameters (maximum pressure and temperature) and its energy performance (power, efficiency), which provides the basis for further design. Clearly from the literature it is evident that only a few researchers [10, 13, 14] have addressed the issues essential to realize the full performance potential of an Ericsson heat pump (or engine).

Building on this limited previous work, this paper aims to propose a revolutionary rotary Ericsson heat pump/engine (REHP), which is a highly efficient, cost effective, scalable and environmentally friendly design. Based on the design, parametric and optimization study has been conducted to evaluate a number of factors affecting the mechanical and thermal performance of the conceptually designed REHP, such as rotor geometries, parts material, porting dimensions, working fluids, base pressure, compression ratio, temperatures and RPM.

2 MACHNISM OF OPERATION AND METHODOLOGY

2.1 Mechanical arrangement and operations

To approach isothermal compression the heat of compression needs to be dissipated rapidly from the compressor chamber and rejected to the heat sink. The general mechanical arrangement shown in Figure 1 indicates a novel compressor design comprising two concentric rotors contained within a circular housing and rotating in the same direction. A compressor and an expander rotor chambers on opposing sides are separated by a recuperator for heat exchange. Each rotor chamber contains a pair of rotors, each rotating while accelerating and decelerating relative to each other, and thus expanding and compressing volumes between the rotors. Each rotor is driven and braked by an independent M-G, which allows the rotation to be optimized. The recuperator shown is a simple counter flow heat exchanger, yet may be shaped and lengthened to minimize pressure drop and maximize heat exchange.

2.2 Rotor cycle rotations

The rotor rotations are shown in sequences A–F in Figure 2, with the expander on the left and compressor on the right of each pair. All rotors are turning counter-clockwise. As the rotors rotate the high- and low-pressure ports are exposed, allowing passage of the working fluid and isolating the compression and expansion segments from the recuperator in a valve-less design.

2.2.1 *Expander*

Following the expander, the red rotor accelerates, expanding the volume behind the red rotor in A–C. In E, the expanded fluid is exposed to the LP port as the blue rotor accelerates and the fluid is transferred out of the expansion chamber in D–F. In D, the volume behind the blue rotor is opened to the high-pressure path of the recuperator and fluid is transferred into the volume. This transfer ends before E and the volume then expands as described before.

2.2.2 *Compressor*

Following the compressor, the volume behind the red rotor is open to the LP port and low-pressure fluid is transferred into the compressor in A. At B, the LP port is closed and the volume behind the red rotor is compressed by the accelerating blue rotor in B and C. In D, the compressed fluid is then exposed to the HP Port and the compressed fluid is transferred into the high-pressure portion of the recuperator. At the same time, the complimentary volume in B–D, the volume behind the blue rotor is open to the LP port and low-pressure fluid is transferred into the volume, which is then compressed in E and F.

A key feature of this design is the large surface areas of the rotors and the casing that allow the heat of compression to be rejected thus allowing the desired, near-isothermal operation.

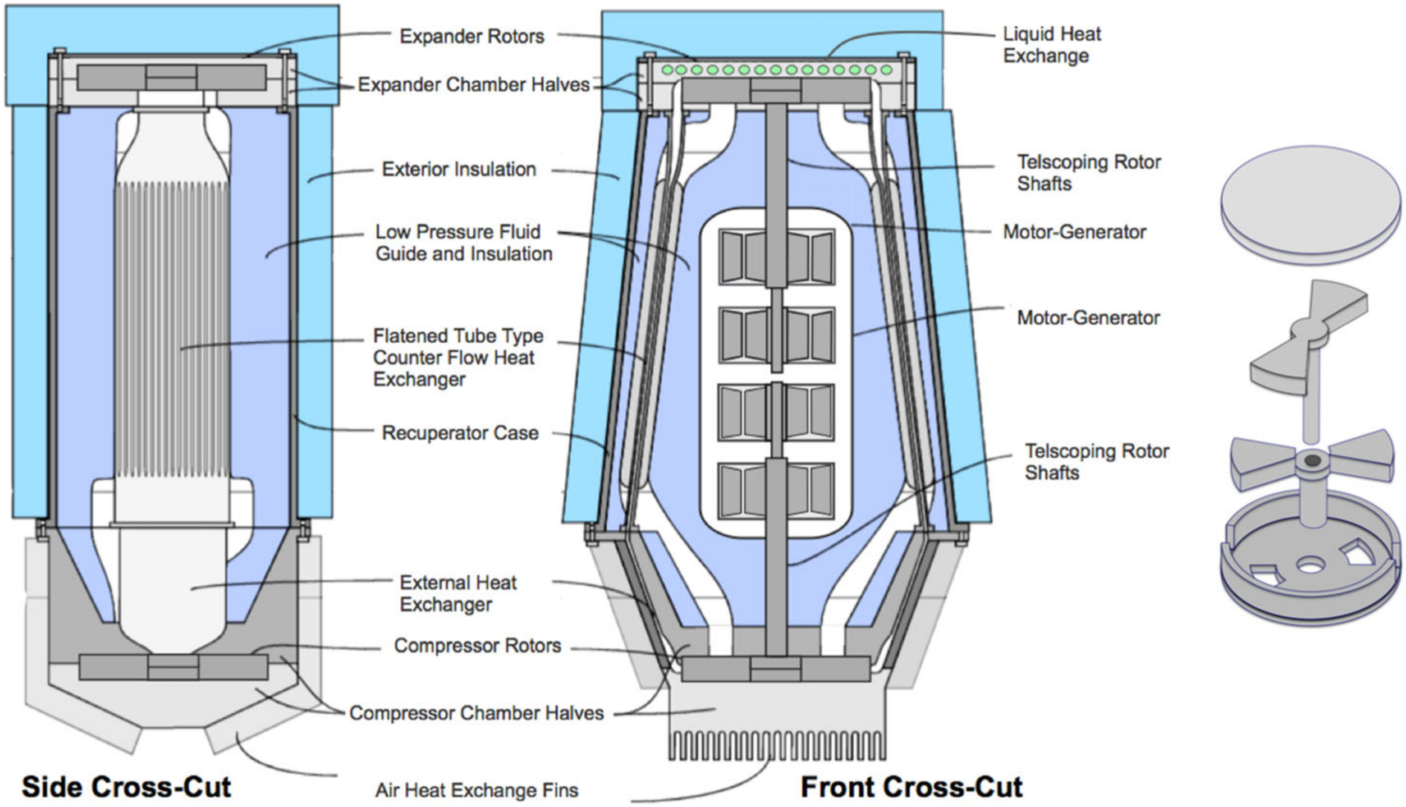

Figure 1. *General mechanical arrangement.*

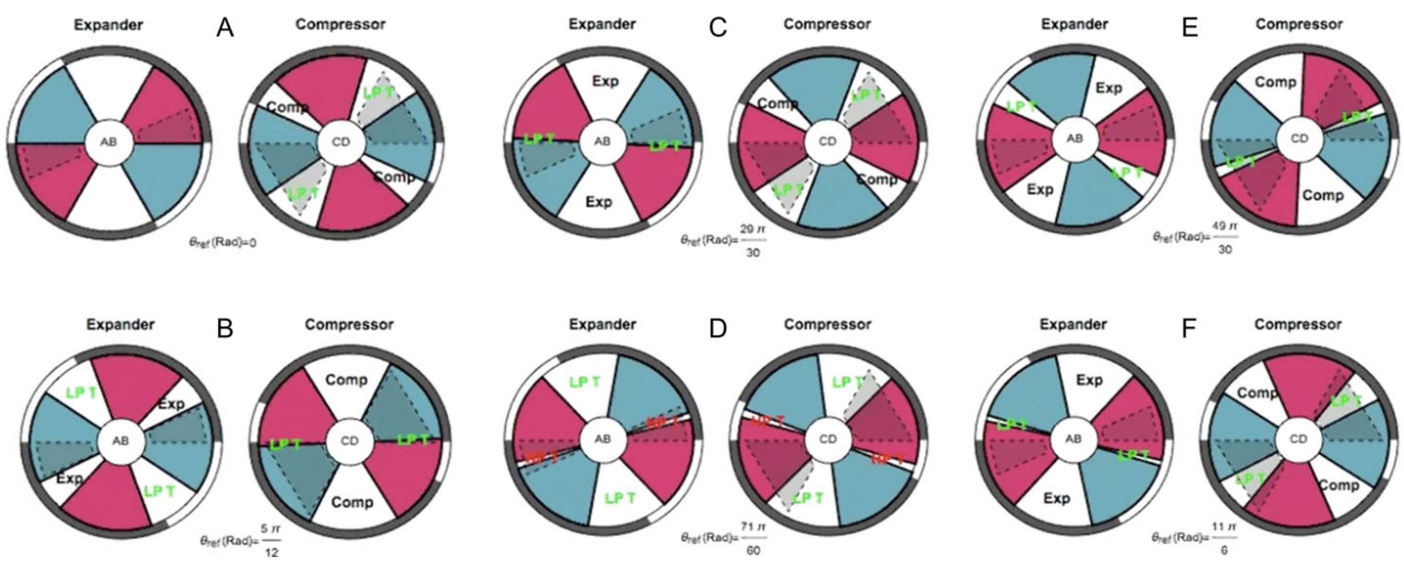

Figure 2. *Rotor cycle rotations.*

2.3 Governing equations

2.3.1 *Rotor motion curve modeling*

The motion of rotor A and rotor B can be described by the following equations:

$$\theta_A = \theta_{\text{ref}} + \text{Amp} \cdot \sin^2\theta_{\text{ref}} \tag{1}$$

$$\theta_B = \theta_{\text{ref}} - \text{Amp} \cdot \sin^2\theta_{\text{ref}} \tag{2}$$

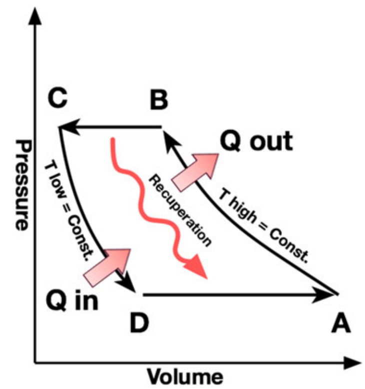

Figure 3. *Ideal Ericsson cycle.*

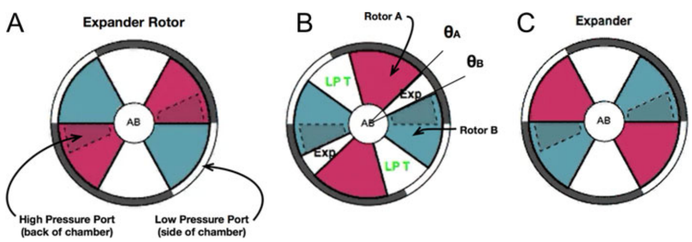

Figure 4. *a: Initial condition. b: start of expansion. c: end of expansion.*

where θ_A and θ_B are the angular positions of the trailing side of rotor A and leading side of rotor B respectively, θ_{ref} is the reference angle and Amp is the amplification factor.

The angular velocity ω, acceleration α for each rotor can be analytically determined as

$$\omega_A = \frac{d\theta_A}{d\theta_{ref}} = 1 + \mathrm{Amp} \cdot \sin(2\theta_{ref}) \tag{3}$$

$$\omega_B = \frac{d\theta_B}{d\theta_{ref}} = 1 - \mathrm{Amp} \cdot \sin(2\theta_{ref}) \tag{4}$$

$$\alpha_A = \frac{d\omega_A}{d\theta_{ref}} = 2\mathrm{Amp} \cdot \cos(2\theta_{ref}) \tag{5}$$

$$\alpha_B = \frac{d\omega_B}{d\theta_{ref}} = -2\mathrm{Amp} \cdot \cos(2\theta_{ref}) \tag{6}$$

2.3.2 *Torque curve modeling*

The torque curves are required by the independently controlled motor-generator as input to get the specific rotor positions as described in (1) and (2).

$$\Sigma\tau = \tau_{MG} + \tau_{WF} + \tau_{ff} = I_s \cdot \alpha \tag{7}$$

$$P_{MG} = 0.105 * \mathrm{RPM} * \tau_{MG}(8)$$

where τ_{MG} is the torque exerted by the motor-generator, τ_{WF} is the torque exerted by the pressure of the working fluid, τ_{ff} is the torque exerted by the frictional force, I_s is the moment of inertia of the rotor system, α is the angular acceleration of the rotors, P_{MG} is the power of the motor-generator and RPM is the number of revolution per minute of the rotors.

2.3.3 *Thermodynamic modeling*

Total mechanical work done in a full closed and ideal Ericsson cycle shown in Figure 3 is

$$\Sigma W_c = W_{AB} + W_{BC} + W_{CD} + W_{DA} \tag{9}$$

where the work done in each segment can be calculated by

$$W_{AB} = P_A \cdot V_A \cdot ln\frac{V_B}{V_A} \tag{10}$$

$$W_{BC} = P_B \cdot (V_C - V_B) \tag{11}$$

$$W_{CD} = P_C \cdot V_C \cdot ln\frac{V_D}{V_C} \tag{12}$$

$$W_{DA} = P_D \cdot (V_A - V_D) \tag{13}$$

2.4 Constraint conditions

The calculations of the rotor motion curves are subjected to the following constraint conditions.

2.4.1 *Initial condition (Figure 4a)*

$t = 0$;
$\theta_{ref} = 0$;
$\theta_A = \theta_B = 0$

This is the start of a reference cycle where the trailing side of rotor A and the leading side of the rotor B are in contact with each other. HP port is just about to open.

2.4.2 *Start of expansion (end of HP transfer) (Figure 4b)*

$$\theta_{AB}(\theta_{ref\_CRV}) = \theta_A - \theta_B = \theta_{AB,\max}/CR$$

where $\theta_{AB,max}$ is the maximum angle between two rotors and CR is the compression ratio; θ_{ref_CRV} can be determined by the above equation.

acrHP $= \theta_B(\theta_{ref\_CRV})$, where arcHP is the opening angle of the HP port.

2.4.3 *End of expansion (start of LP transfer) (Figure 4c)*

$\theta_{AB} = \theta_{AB,max}$

$\theta_{ref,max}|\theta_{AB,max} = \pi/2$

acrRotor $= (\pi - \theta_{AB,max})/2$, where arcRotor is the angle of the rotors.

arcLP = arcRotor, where arcLP is the opening angle of the LP port.

3 RESULTS AND DISCUSSION

3.1 Rotor motion curves

The angular positions, velocities and accelerations of both rotor A and B are illustrated in Figures 5–7. The dimensionless volume between the two rotors is shown in Figure 8 where the volume is normalized by the maximum volume when $\theta_{AB} = \theta_{AB,max}$. As the 'lead' rotor accelerates away from the 'trailing' rotor an increasing volume is created between them, which allows gas to be sucked in through a low-pressure port in the casing end plate. When continued rotation causes the trailing rotor to cut off the suction (LP) port it is then accelerates relative to the leading rotor thus compressing the trapped gas. Further rotation brings the gas into contact with the high-pressure discharge port in the rim of the casing. The trailing rotor continues to move faster than the leading rotor thus causing the gas to be discharged. The trailing rotor is then decelerated relative to the leading rotor thus allowing the volume between to increase again and thus start another suction/compression cycle.

The compressor and expander are designed with two sets of low-pressure and high-pressure ports to allow two cycles per complete 2π rotation. Effectively the combination of the ports and the rotors, electronically controlled to produce the correct timing, provides a valve-less compressor, whose speed can be varied according to the required heat pumping duty.

3.2 Torque curves

The torque curves required by the motor-generator for each rotor are typically illustrated in Figure 9. According to Equation (7), both the torque by working fluid pressure and the rotor acceleration are varying with the reference angle and time. This has resulted in a complex distribution of torque on MG with reference angle at different stages during a complete cycle. Figure 9 has shown that the maximum torque appears at the boundary

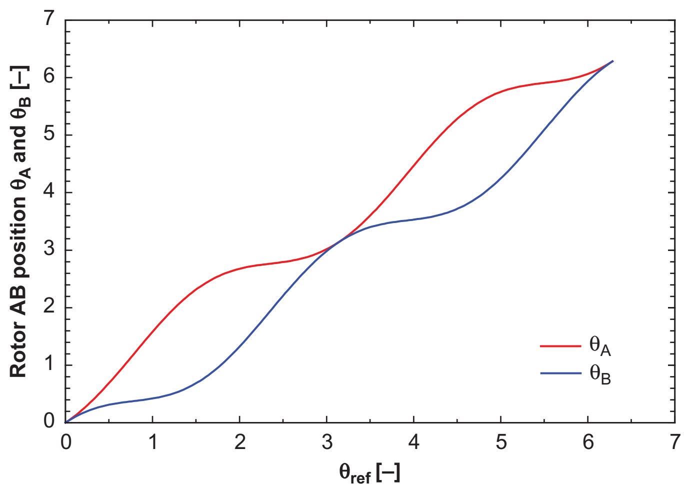

Figure 5. *Angular positions of both rotors.*

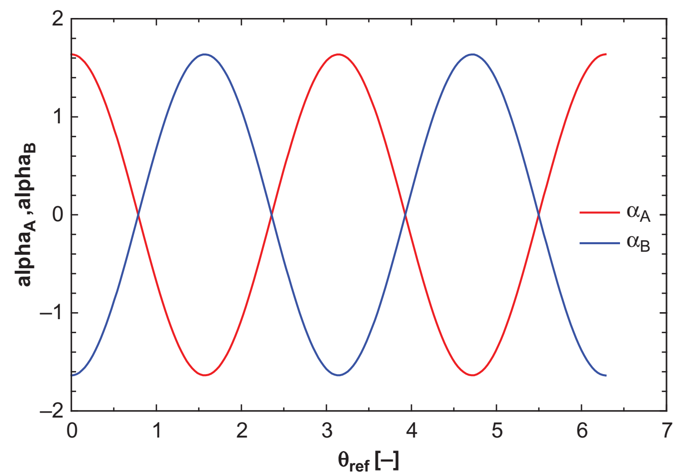

Figure 7. *Angular accelerations of both rotors.*

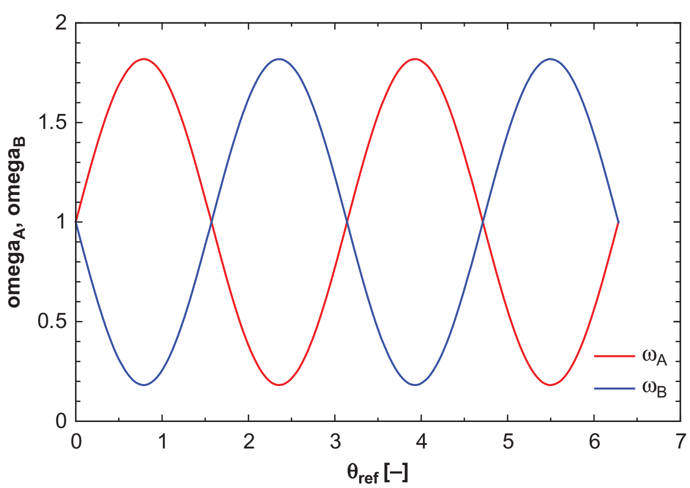

Figure 6. *Angular velocities of both rotors.*

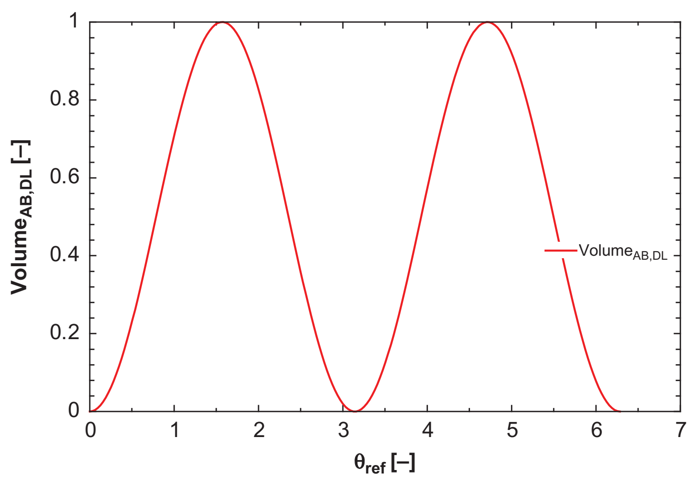

Figure 8. *Dimensionless volume between two rotors.*

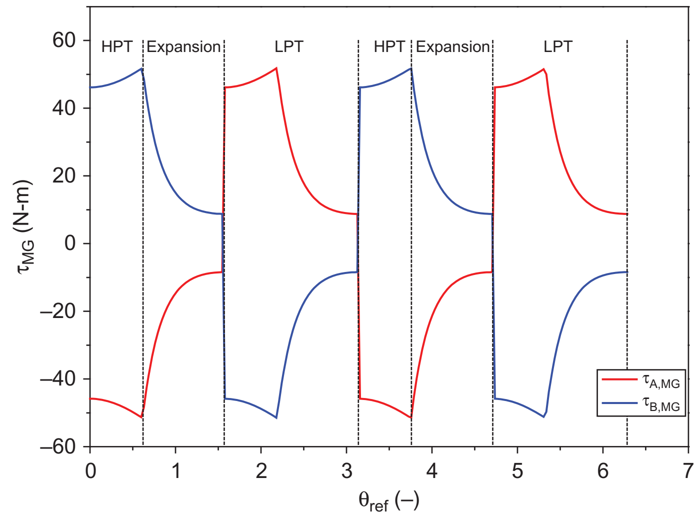

Figure 9. *Torque curves required by the motor-generator.*

Table 1. *Parameters sets used for torque modeling.*

	Set A	Set B
R_r	7 cm	7 cm
R_h	3 cm	3 cm
R_d	2 cm	1 cm
RPM	1000	500
CR	4	3
T_L	273 K	273 K
T_H	700 K	310 K
P_L	400 000 Pa	300 000 Pa

between high-pressure transfer (HPT) and expansion phase. The magnitude of torques on rotors A and B is actually the same, while their directions are opposite. At a specific RPM, the maximum torque and mechanical power obtained from Figure 9 are used for selecting a suitable motor-generator in the market.

3.3 Effects of rotor size and material

Table 1 summarizes two sets of parameters used for the modeling of torque curves, where *R_r* is the outer radius of the rotor, *R_h* is the inner radius of the rotor, *R_d* is the thickness of the rotor, *T_L* is the lower temperature of the expander while *T_H* is the higher temperature of the compressor, *P_L* is the lower pressure of the working fluid at the start of compression.

Using parameters set A in Table 1, the torque curves have been modeled for two different densities of material and the results have been illustrated in Figures 10 and 11. Using parameters set B in Table 1, the results have been illustrated in Figures 12 and 13. The maximum torque on MG is about 43 N-m for a lower density (2700 kg/m^3) rotor and 38 N m for a higher density (6000 kg/m^3) rotor when set A is used. For comparison, the maximum torque on MG is 12.6 N m for a lower density (2700 kg/m^3) rotor and 12.1 N m for a higher density (6000 kg/m^3) rotor when set B is used.

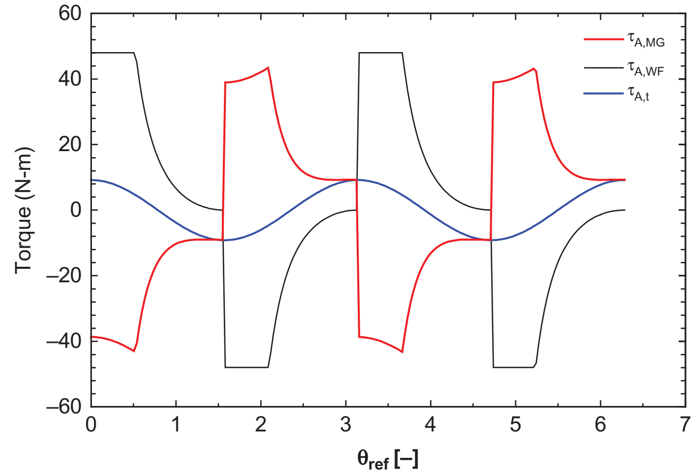

Figure 10. *Torque curves using parameters set A (material density 2700 kg/m^3).*

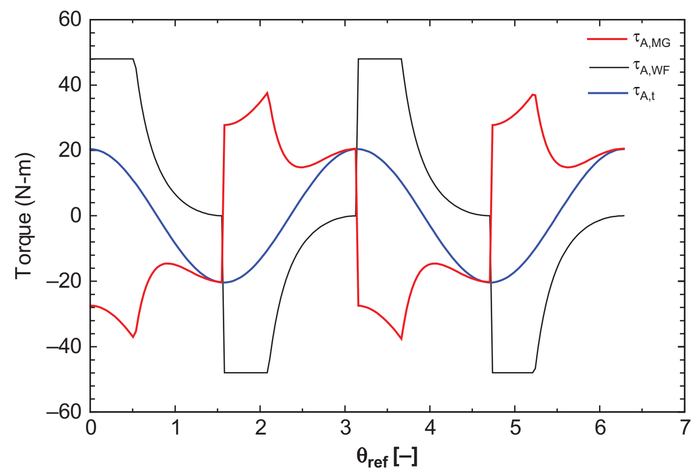

Figure 11. *Torque curves using parameters set A (material density 6000 kg/m^3).*

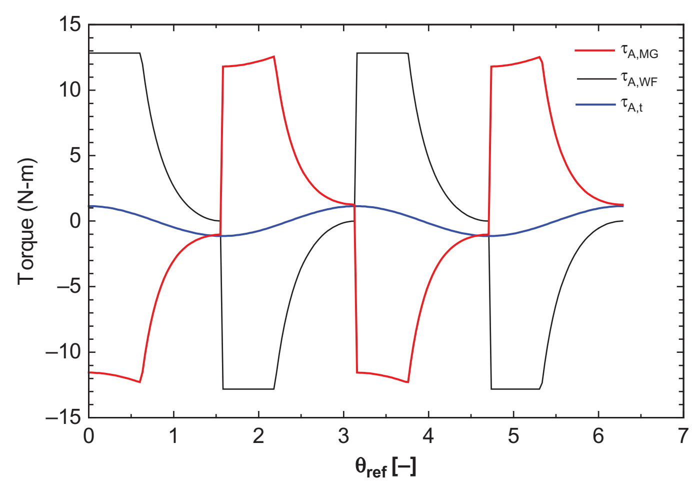

Figure 12. *Torque curves using parameters set B (material density 2700 kg/m^3).*

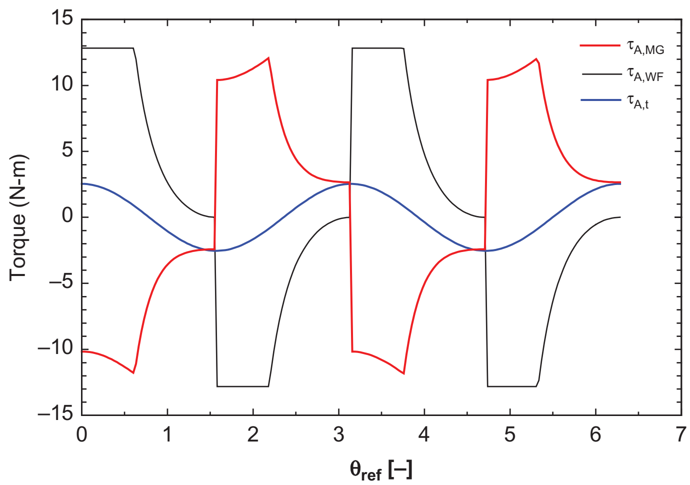

Figure 13. *Torque curves using parameters set B (material density 6000 kg/m³).*

Table 2. *Parametric analysis for a bigger build.*

Bigger build: $R\_r = 10$ cm, $R\_h = 4$ cm, $R\_d = 2$ cm

RPM	CR	P_L (Pa)	Max ericsson power (kW)	τ_{MG_Max} (N m)	Max MG power (W)
500	2	300 000	1.11	25.0	1313
500	3	300 000	1.76	47.5	2494
500	4	300 000	2.22	71.2	3738
500	3	100 000	0.59	13.9	730
500	3	200 000	1.18	30.7	1612
500	3	300 000	1.76	47.5	2494
300	3	300 000	1.06	49.5	1559
400	3	300 000	1.41	48.6	2041
500	3	300 000	1.76	47.5	2494
300	3	100 000	0.35	15.9	501
300	3	200 000	0.70	32.7	1030

It can be found that the effect of the material density on the maximum torque is not significant for both cases. Although higher density leads to high mass and moment of inertia of the rotor, at the moment of maximum torque, the acceleration α is close to 0, which has reduced the effect of the moment of inertia on the overall torque. The dominant term affecting the torque on MG is the torque caused by the working fluid pressure. As for set B, the depth of the rotor has been halved, leading to a much smaller face area and a much lower torque by the working fluid. This has resulted in a much smaller torque on MG. From the practical viewpoint, a smaller torque required by the MG is essential for easier selection of MG with much smaller physical size and lower prices.

3.4 Effects of RPM, CR and base pressure

Parametric analysis has been made for different combinations of RPM, CR and P_L for a bigger build and a small build and the results are summarized in Tables 2 and 3 respectively. To build a laboratory scale prototype of concept, the size of the MG is physically limited, which has led to a limitation of the MG selection in the maximum torque and maximum output power. Therefore, the purpose of the parametric analysis is to find out the best combinations of RPM, CR and P_L and the rotor size. According to the results listed in the above tables, increases in CR and P_L will significantly increase the MG torque and power. The effect of increasing RPM on MG torque and power is less significant. The smaller rotor size in Table 3 is much easier to satisfy a maximum power of the MG to be around 500 W based on the selected ranges of RPM, CR and P_L. However, the build with the bigger rotor size has an advantage in bigger surface area for heat exchange, thus a higher thermal performance. The selection of the rotor size, together with the working conditions needs to be optimized based on a detailed thermodynamic analysis of the system, which is the main research challenge for the next stage.

Table 3. *Parametric analysis for a smaller build.*

Smaller build: $R\_r = 7$ cm, $R\_h = 2.5$ cm, $R\_d = 1$ cm

RPM	CR	P_L (Pa)	Max ericsson power (kW)	τ_{MG_Max} (N m)	Max MG power (W)
500	2	300 000	0.23	6.5	341
500	3	300 000	0.36	12.6	662
500	4	300 000	0.45	18.8	987
500	3	100 000	0.12	4.0	210
500	3	200 000	0.24	8.3	436
500	3	300 000	0.36	12.6	662
300	3	300 000	0.22	12.8	403
400	3	300 000	0.29	12.7	533
500	3	300 000	0.36	12.6	662

4 CONCLUSION

The REHP proposed in this paper has unique advantages over state of the art Rankine and Stirling cycle heat pumps since it can approach Carnot efficiency with the flat rotors maximizing the ratio of the heat exchange surface area to gas volume ratio thus allowing near isothermal compression/expansion. The design is simple, scalable and, with only four moving parts, adaptable to many applications. Efficient switched reluctance motor-generators eliminate mechanical linkage allowing the device to be hermitically sealed. Separate, compression, heat exchanger and expander chambers mean no wasted work on 'dead air', and no thermal creep between parts of the device. Continuous cycling with constant fluid compression, heat exchange and expansion, allows a compact device with high heat pump capacity and efficiency.

Based on the rotor position curves defined in this paper, torque curves are simulated to find out the optimal selection of motor-generator, which is available in the market and also suitable for a laboratory scale build. A number of factors affecting the torque curves have been investigated to identify the most influential ones. The modeling has found that the rotor face area has the largest contribution to the maximum torque required and thus the maximum power of the MG. The rotor size has to been carefully chosen so that the maximum power of the MG fall into a reasonable range while keeping the output power of the system acceptable. Other parameters such as material density, RPM, compression ratio and base pressure have also been studied. It has been found that the rotor material density does not much affect the maximum torque which makes it possible to choose from a wide variety of materials to suit different application needs. Base pressure and compression ratio can have crucial effects on the maximum torque as the torque caused by fluid pressure is much larger than other components of torques caused by moment of inertia or by frictional force.

FUNDING

The authors wish to acknowledge the financial support of the UK Engineering and Physical Sciences Research Council (EPSRC, grant no. EP/P510713/1).

REFERENCES

[1] Legislation.gov.uk. *Climate Change Act 2008*, Chapter 27. http://www.legislation.gov.uk/ukpga/2008/27/pdfs/ukpga_20080027_en.pdf (September 2018, date last accessed).

[2] Samira BD, Ahmed B. Refrigerants and their environmental impact substitution of hydro chlorofluorocarbon HCFC and HFC hydro fluorocarbon. Search for an adequate refrigerant. *Energy Procedia* 2012;**18**: 807–16.

[3] BSRIA (Building Services Research and Information Association). *World Market for Refrigeration (United Kingdom) – A Multi Client Study, by Hugh Brenchley*, 2nd edn, January 2014.

[4] Cengel YA, Boles MA. *Thermodynamics: An Engineering Approach*, 5nd edn. Published by McGraw Hill Higher Education in New York, United States, 2006.

[5] Kaushik SC, Tyagi SK, Bose SK, *et al*. Performance evaluation of irreversible Stirling and Ericsson heat pump cycles. *Int J Therm Sci* 2002;**41**: 193–200.

[6] Toure A, Stouffs P. Modelling of the Ericsson engine. *Energy* 2014;**76**:445–52.

[7] Kaushik SC, Kumar S. Finite time thermodynamic evaluation of irreversible Ericsson and Stirling heat engines. *Energy Convers Manag* 2001;**42**:295–312.

[8] Wojewoda J, Kazimierski Z. Numerical model and investigations of the externally heated valve Joule engine. *Energy*. 2010;**35**:2099–2108.

[9] Kim YM, Shin DKK, Lee JHH A new Ericsson cycle comprising a scroll expander and a scroll compressor for power and refrigeration applications. In *International Refrigeration and Air Conditioning Conference*, 2004, 719.

[10] Carlsen H, Commisso MB, Lorentzen B Maximum obtainable efficiency for engines and refrigerators based on the Stirling cycle. In *Energy Conversion Engineering Conference, IECEC-90. Proceedings of the 25th Intersociety*, 1990, 366.

[11] Hugenroth J, Braun J, King G Liquid-Flooded ericsson cycle cooler: part 1 – thermodynamic analysis. In International Refrigeration and Air Conditioning Conference. 2006, paper R168.

[12] Hugenroth J, Braun J, Groll E, *et al*. Thermodynamic analysis of a liquid-flooded Ericsson cycle cooler. *Int J Refrig* 2007;**30**:1176–86.

[13] Tyagi SK, Kaushik SC, Singhal MK. Parametric study of irreversible Stirling and Ericsson cryogenic refrigeration cycles. *Energy Convers Manag* 2002;**43**:2297–2309.

[14] Kussul E, Makeyev O, Baidyk T, *et al*. Design of Ericsson heat engine with micro channel recuperator. *ISRN Renew Energy*, vol. 2012, Article ID 613642, 8 pages, 2012. https://doi.org/10.5402/2012/613642